

# Characterization of the hydroxypropylmethylcellulose–nicotinamide binary system

Tomoaki Hino<sup>1</sup>, James L. Ford<sup>\*</sup>

*School of Pharmacy and Chemistry, James Parsons Building, Liverpool John Moores University, Byrom Street, Liverpool L3 3AF, UK*

Received 7 September 2000; received in revised form 1 February 2001; accepted 13 February 2001

## Abstract

The effect of hydroxypropylmethylcellulose (HPMC) on the thermal behaviour of nicotinamide was studied. Binary mixtures of nicotinamide and HPMC, composed of various weight fractions of HPMC ( $X_{\text{HPMC}}$ ), were heated, cooled and subsequently re-heated. HPMC dissolved in fused nicotinamide at 140°C. The binary mixture at compositions  $0 \leq X_{\text{HPMC}} \leq 0.3$  formed a film structure on cooling. At  $X_{\text{HPMC}} \geq 0.4$ , the molten nicotinamide at 140°C was saturated with HPMC. These heated mixtures did not form a homogeneous film by cooling to ambient temperature. At  $X_{\text{HPMC}} < 0.4$ , differential scanning calorimetry peaks originating from recrystallization and melting of nicotinamide were observed in the cooling and re-heating scans, respectively. These peaks became smaller with increase in  $X_{\text{HPMC}}$  and disappeared at  $X_{\text{HPMC}} \sim 0.4$ . Decrease in crystallinity with increase in  $X_{\text{HPMC}}$  was confirmed by X-ray diffraction. The glass transition temperature of the cooled mixture ( $T_g$ ) increased with increase in  $X_{\text{HPMC}}$ . When the enthalpy of melting of nicotinamide and  $1/T_g$  were plotted against  $X_{\text{HPMC}}$ , inflections were observed at similar  $X_{\text{HPMC}}$  values, 0.37–0.38. Dissolution of HPMC in molten nicotinamide was accompanied by hydrogen bond formation, which was confirmed by infrared studies. © 2001 Elsevier Science B.V. All rights reserved.

*Keywords:* Nicotinamide; Hydroxypropylmethylcellulose; Differential scanning calorimetry; Hot stage microscopy; Glass transition

## 1. Introduction

Solid dispersions have been extensively investigated for improving the dissolution properties of poorly water-soluble drugs (Ford et al., 1986;

Moneghini et al., 1998; Leuner and Dressman, 2000; Rouchotas et al., 2000). These dispersions are mostly prepared by heating drugs and carriers (Dordunoo et al., 1996; Hülsmann et al., 2000). The method needs control of heating and cooling conditions because of the potential problems of undesirable polymorphic modifications.

Nicotinamide increases the solubilities of nifedipine, indomethacin and halofantrine when formed as solid dispersions with these drugs (Bogdanova et al., 1998; Lim and Go, 2000). Suzuki

<sup>\*</sup> Corresponding author. Tel.: +44-151-2312096; fax: +44-151-2312170.

*E-mail address:* j.l.ford@livjm.ac.uk (J.L. Ford).

<sup>1</sup> Present address: Faculty of Pharmaceutical Sciences, The University of Tokushima, Sho-machi 1-78-1, Tokushima 770-8505, Japan.

and Sunada (1997, 1998), reported that a combination of nicotinamide and hydroxypropylmethylcellulose (HPMC) improved the dissolution properties of nifedipine and nitrendipine. They described that HPMC and nifedipine dissolved in the fused liquid of nicotinamide. In spite of these potential utilities of this combined carrier, the influence of HPMC on the thermal behavior of nicotinamide has yet to be fully investigated.

Recently, Hino et al. (2001) described four polymorphs of nicotinamide. The melting points of Forms I, II, III and IV were 124–134°, 112–117°, 107–111° and ~102°C, respectively. A stable form, Form I was converted to metastable forms, Forms II, III and IV, by melting and recrystallization. The composition of the polymorphs in the recrystallized material depended on the cooling conditions. In the present paper, we report the influence of HPMC on the thermal behavior of nicotinamide.

## 2. Materials and methods

### 2.1. Materials

Reagent grade of nicotinamide was purchased from BDH Laboratories (Poole, UK). HPMC was Methocel E5 premium EP (Colorcon, Dartford, UK). These materials were used without further purification.

### 2.2. Hot stage microscopy and differential scanning calorimetry

Mixtures of nicotinamide and HPMC at various weight fractions were intermixed manually with a mortar and pestle.

For hot stage microscopy (HSM), the physical mixtures of nicotinamide and HPMC were placed on a microscope slide as a small pile. A cover glass was placed on the pile and the thermal behavior of the sample was observed using HSM. The hot stage, the microscope, the central processor and the video cassette recorder of the system used were a Mettler FP82, an Olympus BH-2, a Mettler FP80 and a JVC BR-S920E, respectively. The sample on the glass slide was heated from 30

to 140°C at 10°C min<sup>-1</sup>, laid at ambient temperature (~18°C) by removing the slide from the stage and subsequently heating to 140°C at 10°C min<sup>-1</sup>.

Differential scanning calorimetry (DSC) scans were carried out using a Perkin–Elmer DSC7 calorimeter. Samples ranging from 2.3 to 3.5 mg were placed in aluminum pans and aluminum lids were crimped in position. For scanning, each sample was initially held at 50°C for 1 min, heated to 140°C, held at this temperature for 0.5 min, cooled to -50, 30 or 80°C, held at this temperature for between 0 and 20 min and subsequently re-heated to 140°C. The heating, cooling and re-heating were carried out under the rates as specified in the results section.

### 2.3. X-ray diffraction and infrared studies

Physical mixtures of nicotinamide and HPMC prepared by intermixing with a mortar and pestle were fused at 140°C in an oil bath and cooled to the ambient temperature (resolidified mixtures). Aliquots of the resolidified mixtures were heated to and held at 100°C for 2 h in an oven (re-warmed mixtures). Powder X-ray diffraction patterns and FT-IR spectra of untreated nicotinamide and HPMC, physical, resolidified and re-warmed mixtures were obtained.

Powder X-ray diffraction patterns were obtained by a diffractometer (PW 1729, Philips) at the following conditions; time per step: 1.00 s, step size:  $2\theta = 0.04^\circ$  ( $\theta$ ; incident angle), scanning rate: 1 deg/min, current: 30 mA at 40 kV.

Infrared spectra were obtained from potassium bromide disks ( $\phi = 13$  mm) by an FT-IR spectrometer, Perkin–Elmer 1600 series. Scanning was repeated 16 times.

## 3. Results

### 3.1. Hot stage microscopy observations – dissolution of hydroxypropylmethylcellulose and film formation

Physical mixtures of nicotinamide and HPMC

were heated and subsequently cooled. The photomicrographs of the heated and cooled samples are shown in Fig. 1.

The parameter,  $X_{\text{HPMC}}$ , denotes the weight fraction of HPMC in the mixtures. HPMC dissolved in fused nicotinamide at 140°C at  $X_{\text{HPMC}} \leq 0.3$

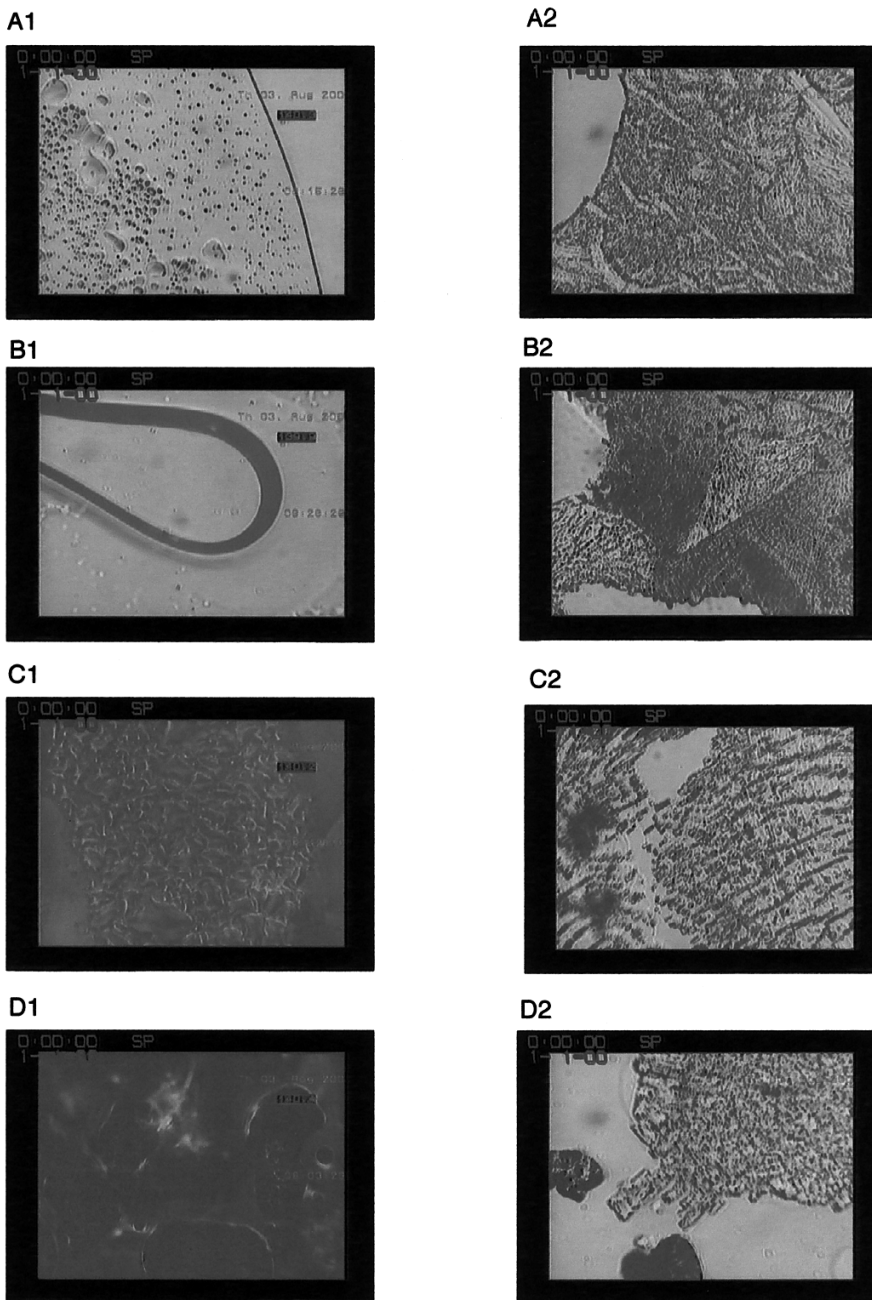


Fig. 1. Photomicrographs of mixtures of HPMC and nicotinamide (A1)–(E1); at 140°C, (A2)–(E2); heated to 140°C and subsequently cooled.  $X_{\text{HPMC}}$ : (A1) and (A2); 0, (B1) and (B2); 0.1, (C1) and (C2); 0.3, (D1) and (D2); 0.4, (E1) and (E2); 0.5.

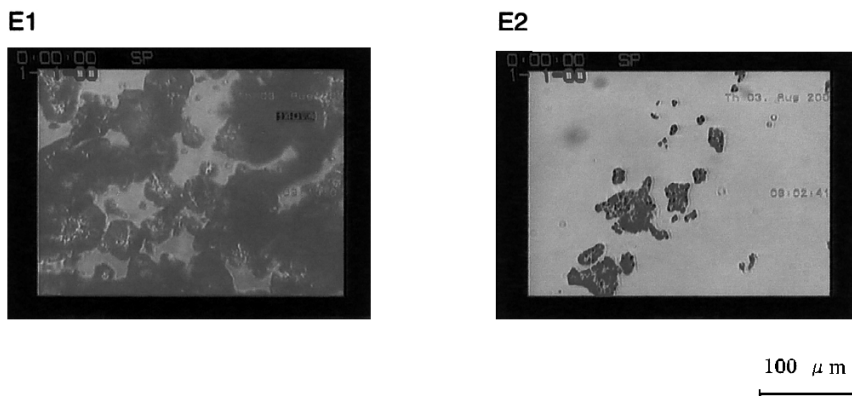


Fig. 1. (Continued)

(Fig. 1 (A1)–(C1)). HPMC partially dissolved and partially remained as particles, resulting in a suspension when  $X_{\text{HPMC}} = 0.4$  (Fig. 1(D1)) Molten nicotinamide was adsorbed on or absorbed into HPMC particles, resulting in a pendular state at  $X_{\text{HPMC}} = 0.5$  (Fig. 1(E1)).

When the heated mixture was cooled to ambient temperature, nicotinamide and HPMC formed films at  $0 \leq X_{\text{HPMC}} \leq 0.3$  (Fig. 1A2–C2). Solid particles and film co-existed at  $X_{\text{HPMC}} = 0.4$  (Fig. 1 (D2)). Powder particles were formed at  $X_{\text{HPMC}} = 0.5$  (Fig. 1(E2)).

The cooled mixtures were re-heated. Recrystallization and melting of the mixtures were observed at 63–110°C and 110–130°C, respectively in the samples of  $0 \leq X_{\text{HPMC}} \leq 0.3$ . Change could not be observed in the samples of  $X_{\text{HPMC}} = 0.4$  or 0.5.

### 3.2. Recrystallization of nicotinamide – differential scanning calorimetry studies

Samples were heated to 140°C, cooled to 30°C and subsequently re-heated to 140°C. The cooling and re-heating scans are shown in Figs. 2 and 3, respectively. A sharp exothermic peak is observed in the cooling scans of nicotinamide. The corresponding enthalpy decreased and the peak was broadened and shifted to the lower temperature with increase in  $X_{\text{HPMC}}$ . The peak disappeared at  $X_{\text{HPMC}}$  of 0.4.

A sharp endothermic peak due to the melting of Form I was observed in the re-heating scan of nicotinamide (Fig. 3). The peak height became lower and the onset temperature decreased with increase in  $X_{\text{HPMC}}$ . Small peaks originating from Forms II and III (Hino et al., 2001) also existed in the re-heating scans. Recrystallization exothermic peaks were observed at 105–116°C in the samples of  $0 \leq X_{\text{HPMC}} \leq 0.3$  (Fig. 3). Melting took place at 103–110°C prior to the recrystallization at  $0.2 \leq X_{\text{HPMC}} \leq 0.3$ . Peaks disappeared at  $X_{\text{HPMC}} = 0.4$ .

The mixtures of HPMC and nicotinamide were heated to 140°C, cooled to 80°C, held at the temperature for 20 min and subsequently re-heated. The DSC re-heating scans are shown in Fig. 4. When untreated nicotinamide without HPMC was cooled under these conditions, the main product was Form II (Hino et al., 2001). Three endothermic peaks due to the melting of Forms IV, III and II were observed at  $X_{\text{HPMC}} = 0.1$ . The peak at  $X_{\text{HPMC}} = 0.2$  originated from Form III. Large peaks originating from Forms I and IV and a small peak from Form III were observed at  $X_{\text{HPMC}} = 0.3$ . Recrystallization caused by solid to solid conversion was observed at this  $X_{\text{HPMC}}$ . No peaks were observed at  $X_{\text{HPMC}} = 0.4$ .

The mixtures of HPMC and nicotinamide were also heated to 140°C, cooled to –50°C, held at this temperature for 10 min and subsequently re-heated. The DSC re-heating scans are shown in

Fig. 5. Recrystallization exotherms appeared in the cooling curves (data not shown) and melting endotherms were observed in the re-heating scans at  $0 \leq X_{\text{HPMC}} \leq 0.3$ . The main endothermic peaks originated from melting of Form I. The enthalpy due to melting decreased with increase in  $X_{\text{HPMC}}$ . Two exothermic peaks existed at 23–50°C and 94–116°C at  $0 \leq X_{\text{HPMC}} \leq 0.3$ . No peaks are observed in either cooling or re-heating scan at  $X_{\text{HPMC}} \geq 0.4$ .

### 3.3. Glass transition of the mixture of nicotinamide and hydroxypropylmethylcellulose

The DSC re-heating scans of Fig. 5 are expanded in Fig. 6. A glass transition was observed in each scan and the transition temperature ( $T_g$ ) increased from  $-6.5$  to  $4.0^\circ\text{C}$  with increase in  $X_{\text{HPMC}}$  from 0 to 0.4. The increase in  $T_g$  to higher temperatures occurred at larger  $X_{\text{HPMC}}$  and the  $T_g$  values at  $X_{\text{HPMC}}$  of 0.7 and 0.9 were  $50.7$  and  $115.6^\circ\text{C}$ , respectively (data not shown).

### 3.4. Powder X-ray study

Fig. 7 shows X-ray diffraction patterns of untreated nicotinamide and HPMC, physical, resoli-

dified and re-warmed mixtures (Fig. 7). Untreated nicotinamide was composed of crystals while HPMC was amorphous (Fig. 7 (a) and (b)).

Although appearance of new peaks or disappearance of the peaks could not be detected in the resolidified nicotinamide (Fig. 7(c)), the peak intensities of the resolidified nicotinamide changed compared with the diffraction pattern of untreated nicotinamide.

To calculate the peak intensity ratios of resolidified to untreated nicotinamide in the three crystal axis directions, Miller indices ( $hkl$ ) were determined. Prior to the determination of Miller indices, the distance ( $d$ ) between the repeating units was calculated by Bragg's equation (Eq. (1)).

$$2d\sin\theta = n\lambda, \quad (1)$$

where  $n$  is an integer, which is an order of the reflection (assigned to 1).  $\lambda$  is the wavelength of  $\text{CuK}\alpha$  ray ( $= 1.542 \text{ \AA}$ ).  $\theta$  is an incident angle.

Miwa et al. (1999) reported the crystal structure of nicotinamide as follows; cell setting: monoclinic, space group:  $p2_1/c$ ,  $z = 4$ ,  $a$ ,  $b$  and  $c$  were  $3.975$ ,  $15.632$  and  $0.422 \text{ \AA}$  (295 K), respectively,  $\beta = 99.03^\circ$  (295 K).

Miller indices ( $hkl$ ) of monoclinic crystals were calculated by Eq. (2).

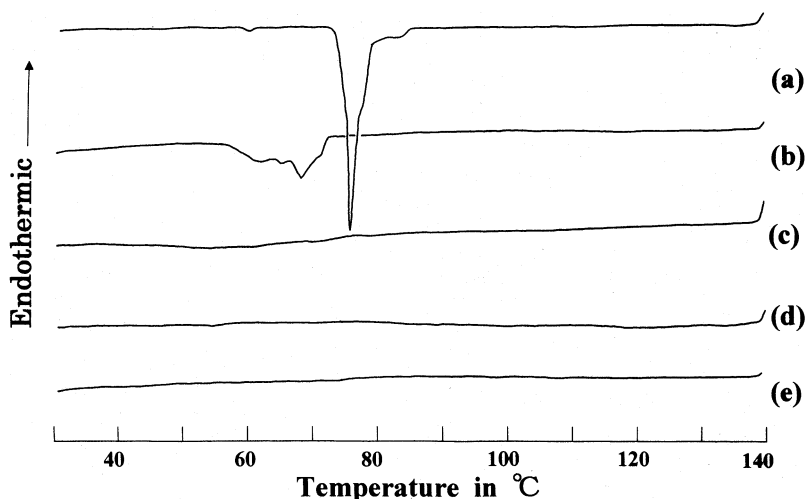


Fig. 2. DSC cooling scans of the mixtures of HPMC and nicotinamide, which had been heated to  $140^\circ\text{C}$ . Heating and cooling rates;  $10^\circ\text{C min}^{-1}$ .  $X_{\text{HPMC}}$ : (a) 0, (b) 0.1, (c) 0.2, (d) 0.3, (e) 0.4.

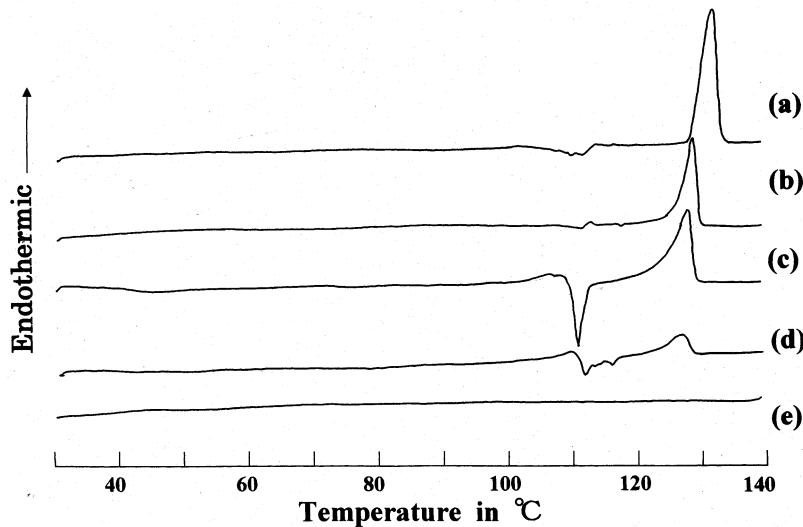


Fig. 3. DSC re-heating scans of the mixtures of HPMC and nicotinamide, which had been heated to 140°C and subsequently cooled to 30°C. Heating, cooling and re-heating rates; 10°C min<sup>-1</sup>.  $X_{\text{HPMC}}$ : (a) 0, (b) 0.1, (c) 0.2, (d) 0.3, (e) 0.4.

$$\frac{1}{d^2} = \left\{ \frac{h^2}{a^2} + \frac{k^2(\sin^2\beta)}{b^2} + \frac{l^2}{c^2} - \frac{2hl(\cos\beta)}{ac} \right\} / \sin^2\beta. \quad (2)$$

The intensities of the (0 2 0) and (1 0 0) reflections (i.e.,  $2\theta = 11.32$  and  $22.65^\circ$ , respectively) increased by 1.73 and 1.33-fold, respectively and the intensity of the (0 0 2) reflection (i.e.,  $2\theta = 19.08^\circ$ ) decreased by 0.29-fold following fusion. Although peak intensity is affected by particle size, filling state in the sample etc., the 1.73- and 0.29-fold changes were large. These results indicate that the crystal habit was modified by fusion and subsequent recrystallization, i.e., growth in the  $b$ -axis direction and inhibition in the  $c$ -axis direction of the crystals.

The crystallinity decreased with increase in  $X_{\text{HPMC}}$  (Fig. 7 (d)–(f)). Although the decrease in the crystallinity of the physical mixture (Fig. 7(d)) is due to the dilution of nicotinamide with HPMC, the crystallinities of resolidified and re-warmed mixtures (Fig. 7 (e)–(g)) decreased more than those of physical mixtures of the same  $X_{\text{HPMC}}$ . The resolidified mixture of  $X_{\text{HPMC}} = 0.3$  was almost amorphous while the crystallinity increased by re-warming at 100°C (Fig. 7(f) and (g)). A new peak caused by fusion and subsequent recrystallization of the binary mixtures was ob-

served at  $2\theta = 17.07^\circ$  at  $X_{\text{HPMC}} = 0.1$  and 0.3 (Fig. 7(e)–(g)).

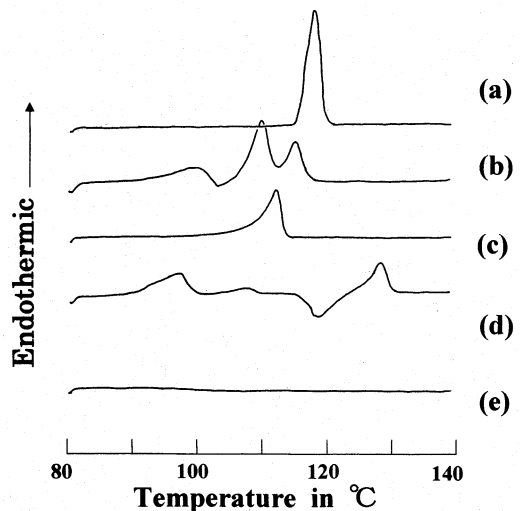


Fig. 4. DSC re-heating scans of the mixtures of HPMC and nicotinamide, which were heated to 140°C and subsequently cooled to and held at 80°C for 20 min. Rates of heating, cooling and re-heating; 20°C min<sup>-1</sup>.  $X_{\text{HPMC}}$ : (a) 0, (b) 0.1, (c) 0.2, (d) 0.3, (e) 0.4.

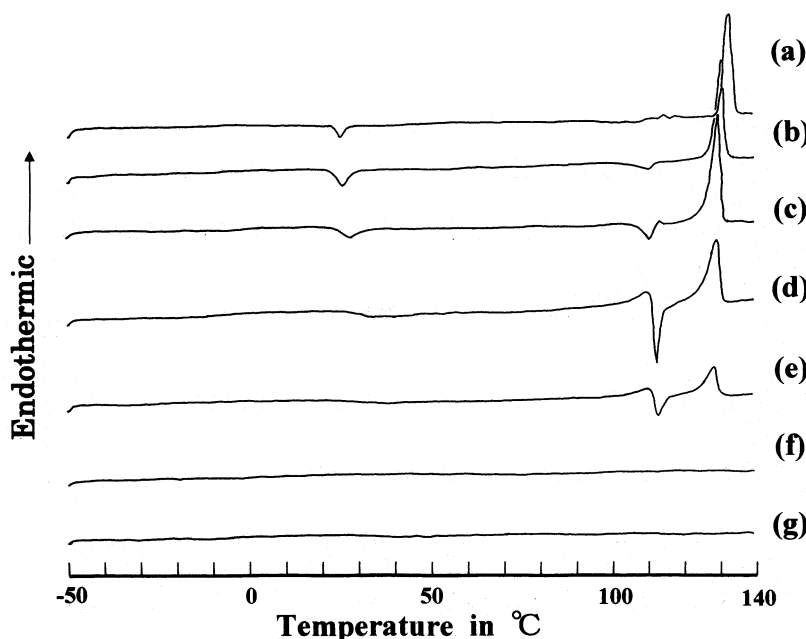


Fig. 5. DSC re-heating scans of the mixtures of HPMC and nicotinamide, which were heated to 140°C and subsequently cooled to and held at  $-50^{\circ}\text{C}$  for 10 min. Heating rate;  $50^{\circ}\text{C min}^{-1}$ , cooling rate;  $200^{\circ}\text{C min}^{-1}$ , re-heating rate;  $20^{\circ}\text{C min}^{-1}$ .  $X_{\text{HPMC}}$ : (a) 0, (b) 0.05, (c) 0.1, (d) 0.2, (e) 0.3, (f) 0.4, (g) 0.5.

## 4. Discussion

### 4.1. Suppression of recrystallization of nicotinamide by hydroxypropylmethylcellulose

HPMC dissolved in fused nicotinamide at  $140^{\circ}\text{C}$  when the weight fraction of HPMC was at  $0 \leq X_{\text{HPMC}} \leq 0.3$  (Fig. 1). Saturation with HPMC in nicotinamide fused at  $140^{\circ}\text{C}$  occurred at  $0.3 < X_{\text{HPMC}} < 0.4$ . Consequently, when the mixture was cooled to ambient temperature, it formed a homogeneous film at  $0 \leq X_{\text{HPMC}} \leq 0.3$  while HPMC particles remained at  $X_{\text{HPMC}} \geq 0.4$ .

HPMC suppressed the recrystallization of nicotinamide under the conditions when either Form I (Figs. 2, 3, 5 and 7) or Form II (Fig. 4) was formed when only nicotinamide without HPMC was cooled (Hino et al., 2001). The DSC peak height was reduced with increase in  $X_{\text{HPMC}}$  and disappeared at  $X_{\text{HPMC}} \geq 0.4$ .

The enthalpy of the main endothermic peak in Fig. 5 per unit weight ( $\Delta H$ ) was plotted against

$X_{\text{HPMC}}$  (Fig. 8).  $\Delta H$  linearly decreased with increase in  $X_{\text{HPMC}}$ . The regression line was expressed by Eq. (3) (correlation coefficient:  $-0.993$ ,  $n = 5$ ).

$$\Delta H = -578.9 X_{\text{HPMC}} + 221.0. \quad (3)$$

The intercept of the regression line on the abscissa was 0.38. The value is between 0.3 and 0.4, in the region where the fused nicotinamide is saturated with HPMC (Fig. 1) and peaks disappeared in the DSC cooling and re-heating scans (Figs. 2–5).

HPMC does not melt in the temperature region  $\leq 140^{\circ}\text{C}$  (Ford, 1999). The endothermic peak represents the melting of nicotinamide and concomitant dissolution of HPMC. If nicotinamide did not molecularly interact with HPMC, HPMC and fused nicotinamide liquid saturated with HPMC would exist separately at  $X_{\text{HPMC}} \geq 0.4$ . In this case, the endothermic peak of nicotinamide would not disappear at  $0 \leq X_{\text{HPMC}} < 1$  and the intercept of the line on the abscissa in Fig. 8 would be unity because  $\Delta H$  is considered to be proportional to

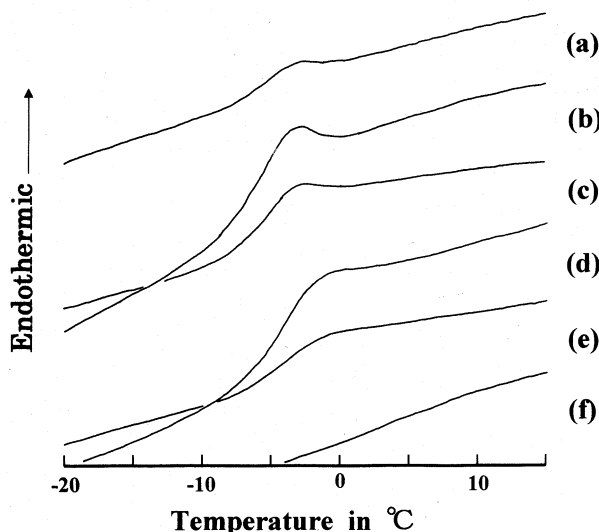


Fig. 6. Expanded DSC re-heating scans of Fig. 5.  $X_{\text{HPMC}}$ : (a) 0, (b) 0.05, (c) 0.1, (d) 0.2, (e) 0.3, (f) 0.4.

the weight fraction of nicotinamide in the mixture (i.e.,  $1 - X_{\text{HPMC}}$ ). However, the peak disappeared at  $0.3 < X_{\text{HPMC}} < 0.4$  and the intercept is 0.38. Therefore, the suppression of recrystallization of nicotinamide with HPMC is due to not only the dilution effect of HPMC but also to molecular

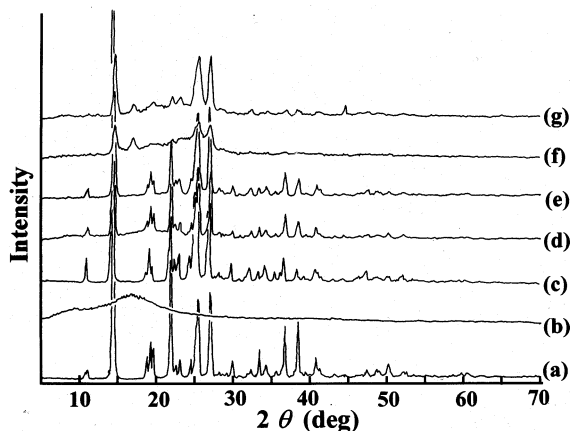


Fig. 7. Powder X-ray diffraction patterns of untreated nicotinamide and HPMC, physical, resolidified and re-warmed mixtures. (a) untreated nicotinamide, (b) HPMC, (c) resolidified nicotinamide, (d) physical mixture, (e) and (f) resolidified mixtures, (g) re-warmed mixture.  $X_{\text{HPMC}}$ : (d) 0.3, (e) 0.1, (f) and (g) 0.3.

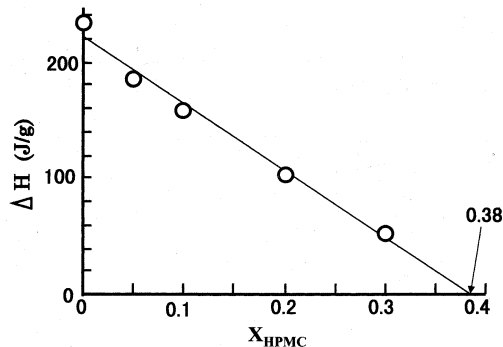


Fig. 8. Relationship between the enthalpy  $\Delta H$  of the endothermic peak of the re-heating curve (Form I) and  $X_{\text{HPMC}}$ .

interaction between nicotinamide and HPMC. A different molecular interaction mechanism would be considered between the HPMC-low concentration mixtures ( $0 \leq X_{\text{HPMC}} \leq 0.3$ ) and high concentration mixtures ( $X_{\text{HPMC}} \geq 0.4$ ). The suppression of recrystallization of nicotinamide by the molecular interaction with HPMC might reduce the intermolecular bonds of nicotinamide in solid dispersions. Consequently, the binary mixtures improved the dissolution properties of poorly water-soluble drugs (Suzuki and Sunada, 1997, 1998).

#### 4.2. Intermolecular formation of hydrogen bonds between nicotinamide and hydroxypropylmethylcellulose

Although a cooling rate of  $200^\circ\text{C min}^{-1}$  used in Figs. 5 and 6 was not completely controllable, the intention of adopting this rate of cooling samples was to cool as rapidly as possible in order to obtain the glassy state that could not be produced with nicotinamide alone (Hino et al., 2001). However, recrystallization peaks appeared in the cooling scans and melting peaks were observed in the re-heating scans at  $0 \leq X_{\text{HPMC}} \leq 0.3$  above the  $T_g$ . The glass transition was observed in the re-heating scans of all samples. Therefore, the cooled samples at  $0 \leq X_{\text{HPMC}} \leq 0.3$  are considered to be composed of crystalline and glassy moieties. The samples at  $X_{\text{HPMC}} \geq 0.4$  were amorphous.

The  $T_g$  of a film formed from two components may be described by Eq. (4) (Nielson, 1974; Timko and Lordi, 1979).



$$1/T_g = X_a/T_{ga} + X_b/T_{gb}, \quad (4)$$

where the subscripts a and b denote the two components.  $X_a$  and  $T_{ga}$  are the weight fraction and the glass transition temperature of the component a. The corresponding values of the component b are  $X_b$  and  $T_{gb}$ . Consequently, the transition temperature of the present system is represented by Eq. (5).

$$1/T_g = (1/T_{g\text{HPMC}} - 1/T_{g\text{NA}})X_{\text{HPMC}} + 1/T_{g\text{NA}}, \quad (5)$$

where  $T_{g\text{HPMC}}$  and  $T_{g\text{NA}}$  are the glass transition temperatures of HPMC and nicotinamide, respectively. At the region of  $0 \leq X_{\text{HPMC}} \leq 0.3$ , the regression line was represented by Eq. (6) (correlation coefficient:  $-0.984$ ,  $n = 5$ ) (Fig. 9).

$$1/T_g = -0.000126 X_{\text{HPMC}} + 0.00372. \quad (6)$$

At the region of  $0.4 \leq X_{\text{HPMC}} \leq 0.9$ , the regression line was represented by Eq. (7) (correlation coefficient:  $-0.993$ ,  $n = 4$ ) (Fig. 9).

$$1/T_g = -0.00201 X_{\text{HPMC}} + 0.00442. \quad (7)$$

$X_{\text{HPMC}}$  at the cross point of the two regression lines is 0.37, which coincided with the intercept of the enthalpy line on the abscissa in Fig. 8. The weight ratio of HPMC: nicotinamide at this  $X_{\text{HPMC}}$  denotes that one residue of HPMC bound to 2.7 nicotinamide molecules. The summation of the average number of hydroxyl and hydroxypro-

poxyl groups per one HPMC residue is  $\sim 2.1$ . The similarity of the two values indicates that the dissolution of HPMC into nicotinamide is mainly due to the hydrogen bonding of nicotinamide to the hydroxyl and hydroxypropoxyl groups of HPMC. The slight difference values suggest that nicotinamide molecules bound to the surface of the HPMC particles not dissolved by the molten liquid. This effect of hydrogen bonding between the adsorbed nicotinamide and the surface of the particles on increase in the binding ratio is considered to be significant, taking into the fact that the steric hindrance of dissolved HPMC random coils might lower the ratio.

Fig. 10 shows FT-IR spectra of nicotinamide (Fig. 10(a) and (b)), HPMC (Fig. 10 (c)) and binary mixtures (Fig. 10(d) and (e)). Fusion of nicotinamide did not induce major peak shifts (Fig. 10(b)).

The peak originating from N–H stretching was shifted from  $3161 \text{ cm}^{-1}$  of untreated nicotinamide (Fig. 10(a)) to  $3165 \text{ cm}^{-1}$  at  $X_{\text{HPMC}} = 0.1$  and  $0.3$  (Fig. 10(d) and (e)). This change indicates the formation of hydrogen bonds between nicotinamide and HPMC. The peak at  $1422 \text{ cm}^{-1}$  of untreated nicotinamide shifted to  $1424 \text{ cm}^{-1}$  at  $X_{\text{HPMC}} = 0.1$  and  $0.3$ , which presumably represents the deformation of pyridine ring structure due to the formation of hydrogen bonds. The peak shapes of resolidified mixtures about  $1020$ –

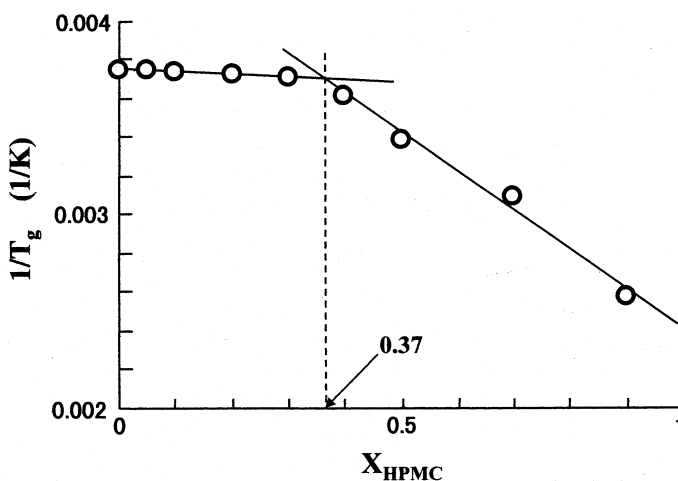


Fig. 9. Relationship between  $1/T_g$  and  $X_{\text{HPMC}}$ .

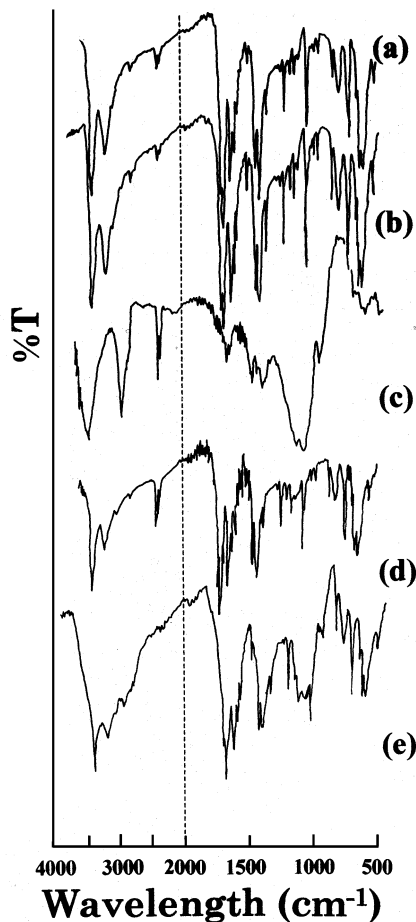


Fig. 10. FT-IR spectra of nicotinamide, HPMC and binary mixtures. (a) untreated nicotinamide, (b) resolidified nicotinamide, (c) HPMC, (d) and (e) resolidified mixtures.  $X_{\text{HPMC}}$ : (d) 0.1, (e) 0.3.

1150 and  $3100\text{--}3400\text{ cm}^{-1}$  broadened compared to the untreated nicotinamide and the equivalent physical mixtures. These results indicate the restriction of vibration due to hydrogen bonding. These FT-IR studies confirmed the intermolecular forma-

tion of hydrogen bonds between nicotinamide and HPMC.

#### 4.3. Percolation threshold of the binary mixture composed of nicotinamide and hydroxypropylmethylcellulose

The  $T_g$  of nicotinamide calculated by Eq. (6) is  $-4.5^\circ\text{C}$ , which is similar to the experimental value of  $-6.5^\circ\text{C}$ . The value of HPMC calculated with Eq. (7) is  $142^\circ\text{C}$ , which is similar to the literature value of  $153\text{--}180^\circ\text{C}$  (Sakellariou and Rowe, 1995).

In the region of  $0 \leq X_{\text{HPMC}} < 0.37$ , HPMC dissolved in molten nicotinamide. The effect of nicotinamide on the characteristics of this range of binary system is predominant. In the region of  $X_{\text{HPMC}} > 0.37$ , molten nicotinamide solution saturated with HPMC was probably adsorbed by HPMC particles and penetrated into the inner portion of the particles. Molten nicotinamide might act as a binder liquid for the excess HPMC particles. When the excess was small ( $X_{\text{HPMC}} = 0.4$ ), the system was in a suspension state. The system became pendular ( $X_{\text{HPMC}} = 0.5$ ), presumably via the funicular state, with increase in  $X_{\text{HPMC}}$ , because the degree of aggregation decreased with decrease in the amount of binder liquid binding the HPMC particles. The influence of the HPMC particles on the characteristics of the binary system became more predominant with the increase in  $X_{\text{HPMC}}$ . Therefore, the experimental  $T_{g\text{HPMC}}$  value became similar to the literature values. This change in  $T_g$  of the binary mixture at  $X_{\text{HPMC}}$  of  $\sim 0.37$  is considered to be caused by a percolation and this critical  $X_{\text{HPMC}}$  value is the percolation threshold (Bony and Leuenberger, 1991; Leu and Leuenberger, 1993; Caraballo et al., 1999).

Percolation theory might explain the physical properties of the binary mixtures composed of nicotinamide and HPMC. In this theory, physical properties of the system,  $Y$ , are expressed as Eq. (8).

Table 1

Physical properties of the binary mixture composed of nicotinamide and HPMC expressed by the form of Eq. (8)

$X_{\text{HPMC}}$	$\Delta H$ (J/g)	$1/T_g$ ( $\text{K}^{-1}$ )
$0 \leq X_{\text{HPMC}} \leq 0.3$	$\Delta H = -579 (X_{\text{HPMC}} - 0.38)$	$1/T_g - 0.00368 = -0.000126 (X_{\text{HPMC}} - 0.37)$
$0.4 \leq X_{\text{HPMC}} \leq 1$	$\Delta H = 0 (X_{\text{HPMC}} - 0.38) = 0$	$1/T_g - 0.00368 = -0.00201 (X_{\text{HPMC}} - 0.37)$

$$Y - Y_c = S(X - X_c)^p \quad (8)$$

where  $X$  is the weight fraction of a certain component.  $X_c$  is the weight fraction at the percolation threshold.  $Y_c$  is correction term.  $S$  and  $p$  are scaling factor and critical exponent, respectively.

By rearranging Eqs. (3), (6) and (7),  $\Delta H$  and  $1/T_g$  of the binary mixtures composed of nicotinamide and HPMC are expressed by the form of Eq. (8) (Table 1). Two different physical properties of the mixtures, i.e.,  $\Delta H$  and  $1/T_g$ , had similar percolation thresholds ( $\approx 0.37$ ).

Nicotinamide molecules form intermolecular hydrogen bonds as N2H...O1 and N2H...N1 in their crystals. The crystal structure consists of molecules stacking along the  $a$ -axis and the planar pyridine rings are in contact with a plane-to-plane distance of 3.58 Å (Miwa et al., 1999). At much smaller  $X_{\text{HPMC}}$  values than the threshold, nicotinamide molecules interacted with each other by hydrogen bonding and  $\pi$ - $\pi$  interactions and surrounded the HPMC molecules. The network composed of nicotinamide molecules was predominant in the binary mixtures. Consequently, the mixtures were molten at 140°C and formed films on cooling. As  $X_{\text{HPMC}}$  increased in the range  $0 < X_{\text{HPMC}} < 0.37$ , the intermolecular hydrogen bonds between nicotinamide molecules, which constructed the network of nicotinamide crystals, were replaced by intermolecular hydrogen bonds between nicotinamide and HPMC molecules, resulting in a linear decrease in  $\Delta H$  (Fig. 8). In this  $X_{\text{HPMC}}$  range, some nicotinamide molecules interacted with other nicotinamide molecules and HPMC ones by hydrogen bonding and the network constructed of hydrogen bonding between nicotinamide molecules still remained.

At the larger  $X_{\text{HPMC}}$  values than the threshold (the range of  $X_{\text{HPMC}} > 0.37$ ), the network could not be constructed with nicotinamide molecules, resulting in disappearance of the melting and recrystallization peaks in the DSC scans. Nicotinamide was in a glassy state in the heated and subsequently cooled mixtures because nicotinamide molecules were presumably adsorbed and percolated into the inner part of HPMC particles.

## References

- Bogdanova, S., Sidzhakova, D., Karaivanova, V., Georgieva, S., 1998. Aspects of the interactions between indomethacin and nicotinamide in solid dispersions. *Int. J. Pharm.* 163, 1–10.
- Bony, J.D., Leuenberger, H., 1991. Matrix type controlled release systems. I. Effect of percolation on drug dissolution kinetics. *Pharm. Acta Helv.* 66, 160–164.
- Caraballo, I., Melgoza, L.M., Alvarez-Fuentes, J., Soriano, M.C., Rabasco, A.M., 1999. Design of controlled release inert matrices of naltrexone hydrochloride based on percolation concepts. *Int. J. Pharm.* 181, 23–30.
- Dordunoo, S.K., Ford, J.L., Rubinstein, M.H., 1996. Solidification studies of polyethylene glycols, gelucire 44/14 or their dispersions with triamterene or temazepam. *J. Pharm. Pharmacol.* 48, 782–789.
- Ford, J.L., 1999. Thermal analysis of hydroxypropylmethylcellulose and methylcellulose: powders, gels and matrix tablets. *Int. J. Pharm.* 179, 209–228.
- Ford, J.L., Stewart, A.F., Dubois, J.-L., 1986. The properties of solid dispersions of indomethacin or phenylbutazone in polyethylene glycol. *Int. J. Pharm.* 28, 11–22.
- Hino, T., Ford, J.L., Powell, M.W., 2001. Assessment of nicotinamide polymorphs by differential scanning calorimetry. *Thermochim. Acta*, submitted for publication.
- Hülsmann, S., Backensfeld, T., Keitel, S., Bodmeier, R., 2000. Melt extrusion – an alternative method for enhancing the dissolution rate of 17-estradiol hemihydrate. *Eur. J. Pharm. Biopharm.* 49, 237–242.
- Leu, R., Leuenberger, H., 1993. Application of percolation theory to the compaction of pharmaceutical powders. *Int. J. Pharm.* 90, 213–219.
- Leuner, C., Dressman, J., 2000. Improving drug solubility for oral delivery using solid dispersions. *Eur. J. Pharm. Biopharm.* 50, 47–60.
- Lim, L.-Y., Go, M.-L., 2000. Caffeine and nicotinamide enhances the aqueous solubility of the antimalarial agent halofantrine. *Eur. J. Pharm. Sci.* 10, 17–28.
- Miwa, Y., Mizuno, T., Tsuchida, K., Taga, T., Iwata, Y., 1999. Experimental charge density and electrostatic potential in nicotinamide. *Acta Crystallograph. (B)* 55, 78–84.
- Moneghini, M., Carcano, A., Zingone, G., Perissutti, B., 1998. Studies in dissolution enhancement of atenolol. Part I. *Int. J. Pharm.* 177–183.
- Nielson, L.E., 1974. *Mechanical Properties of Polymers and Composite*, vol. 1. Dekker, New York, p. 25.
- Rouchotas, R., Cassidy, O.E., Rewley, G., 2000. Comparison of surface modification and solid dispersion techniques for drug dissolution. *Int. J. Pharm.* 195, 1–6.
- Sakellariou, P., Rowe, R.C., 1995. Interactions in cellulose derivative films for oral drug delivery. *Prog. Polym. Sci.* 20, 889–942.
- Suzuki, H., Sunada, H., 1997. Comparison of nicotinamide, ethylurea and polyethylene glycol as carriers for nifedipine solid dispersion systems. *Chem. Pharm. Bull.* 45, 1688–1693.
- Suzuki, H., Sunada, H., 1998. Some factors influencing the dissolution of solid dispersions with nicotinamide and hydroxypropylmethylcellulose as combined carriers. *Chem. Pharm. Bull.* 46, 1015–1020.
- Timko, R.J., Lordi, N.G., 1979. Thermal characterization of citric acid and solid dispersions with benzoic acid and phenobarbital. *J. Pharm. Sci.* 68, 601–605.